Multiconfigurational quantum propagation with trajectory-guided generalized coherent states

Adriano Grigolo[a]

Instituto de Física Gleb Wataghin, Universidade Estadual de Campinas,

777 Sérgio Buarque de Holanda, 13083-859, Campinas,

Brazil

Thiago F. Viscondi[b]

Instituto de Física, Universidade de São Paulo, 1371 Rua do Matão, 05508-090,

São Paulo, Brazil

Marcus A. M. de Aguiar[c]

Instituto de Física Gleb Wataghin, Universidade Estadual de Campinas,

777 Sérgio Buarque de Holanda, 13083-859, Campinas,

Brazil

(Dated: 4 February 2016)

A generalized version of the coupled coherent states method for coherent states of arbitrary Lie groups is developed. In contrast to the original formulation, which is restricted to frozen-Gaussian basis sets, the extended method is suitable for propagating quantum states of systems featuring diversified physical properties, such as spin degrees of freedom or particle indistinguishability. The approach is illustrated with simple models for interacting bosons trapped in double- and triple-well potentials, most adequately described in terms of SU(2) and SU(3) bosonic coherent states, respectively.

---

[a] Electronic mail: agrigolo@ifi.unicamp.br

[b] Electronic mail: viscondi@if.usp.br

[c] Electronic mail: aguiar@ifi.unicamp.br

I. INTRODUCTION

A vast number of physical systems exhibit the property that some of their parts behave in a sort of classical way, meaning that quantum effects play only a minor role in the description of those parts. This distinctive classical character of specific degrees of freedom is a much welcomed attribute, for it makes possible the development of tractable computational approaches capable of carrying out the time-evolution of complex quantum systems, being thus the fundamental property upon which time-dependent trajectory-guided methods are based.

In this kind of technique quantum states are represented in terms of time-dependent basis functions or 'configurations'. Within a single configuration, those degrees of freedom in which quantum effects are negligible are evolved according to classical equations of motion. This classical dynamics may be prescribed in a number of different ways and different choices correspond to different propagation schemes.

In spite of the fact that individual configurations have some of their parts bound to obey classical laws, a complete quantum solution is in principle attainable by combining many configurations. The key idea behind such 'multiconfigurational' approaches is that trajectory-guided basis functions are more likely to remain in the important regions of the Hilbert space, thus being more efficient at representing the quantum state in the sense that a reduced number of basis elements is required in order to achieve an accurate description. And it is precisely through a significant reduction in the number of basis functions needed to propagate the system that one hopes to escape the exponential scaling of basis-set size with dimensionality typical of standard static-basis formulations. This 'mixed quantum-classical' picture is adopted in many methods of quantum chemistry.[1]

A recurrent theme in this field is the development of techniques which, by means of equally simple recipes to guide the basis functions, would be readily applicable to systems presenting authentically non-classical qualities, such as spin degrees of freedom or particle exchange symmetry. Several works have been directed to that purpose, most often aiming at a time-dependent description of the electronic structure of molecules during non-adiabatic processes. One particular example of such a recipe is the classical model for electronic degrees of freedom proposed by Miller and White[2] in which a second-quantized fermionic Hamiltonian is properly reduced to a classical function wherein number and phase variables

2

play the role of generalized coordinates. In contrast, a more 'mechanistic' approach to fermion dynamics is found on the multiconfigurational formula proposed by Kirrander and Shalashilin[3] in which the basis functions consist of antisymmetrized frozen Gaussians[5] guided by fermionic molecular dynamics.[6]

Yet if one seeks to describe non-classical degrees of freedom by means of classical-like variables, then generalized coherent states – defined in the group-theoretical sense – are indisputably the most appropriate tools to be employed. There are many reasons supporting this assertion.

First of all, coherent states are defined in terms of non-redundant parameters and equations of motion for these parameters can be readily obtained from the time-dependent variational principle. In this way an optimized time-evolution can be assigned in an unambiguous manner. Moreover, they are naturally able to capture the desired symmetries of the system which are maintained during propagation. Furthermore, the coherent-state parameters evolve in a classical phase space in the strict sense of the word, hence we automatically have at our disposal the wealth of analytical techniques applicable to Hamiltonian systems. At the same time, through this intimate connection to classical dynamics, coherent states provide a compelling classical interpretation to quantum phenomena, in so far as individual configurations are chosen to represent familiar objects – i.e. in such a way that it is meaningful to discuss the dynamics of the system in terms of their trajectories. To this extent, coherent states – which are also minimum uncertainty states (provided a proper meaning is assigned to the term 'uncertainty') – are valuable tools in enhancing our comprehension with respect to the semiclassical features of the quantum system under investigation. In addition, the group-theoretical formalism secures a well-defined integral form for the coherent-state closure relation – a crucial element to the developments hereby presented. This list of virtues is not exhausted and other advantages of a generalized coherent-state representation will be pointed out throughout the paper.

Along these lines, Van Voorhis and Reichman[7] have considered a number of alternative representations of electronic structure making use of different coherent-state parametrizations and also examined their adequacy to a variety of systems.[11] Within the context of nonadiabatic molecular dynamics, a particularly interesting coherent-state representation[12,13] is found in the simplest and most throughly investigated version of the Electron-Nuclear Dynamics theory, developed by Deumens, Öhrn and collaborators.[14,15] The same kind of

coherent state has been discussed in detail, within the field of nuclear physics, by Suzuki and Kuratsuji.[16–18] Turning to bosonic dynamics, a semiclassical trajectory-based formula in the $SU(n)$ coherent-state representation has been recently derived and successfully applied to a model of trapped bosons.[19,20]

These methods are representative of the kind of technique one has in mind when a description of intrinsically quantum degrees of freedom in terms of classical-like variables is desired. However, they either constitute approximate single-configuration approaches[14,15] or involve complicated trajectories that live in a duplicated phase space,[19,20] sometimes relying on sophisticated root-search techniques in order to determine them.[7,21,22] It seems that a multiconfigurational, generalized coherent-state approach, based on simple – as opposed to duplicated – phase-space trajectories would be more in the spirit of the familiar time-dependent guided-basis methods of quantum chemistry.[23] This is precisely the direction we take here.

In this work a quantum initial value representation method which employs a generalized coherent-state basis set guided by classical trajectories is formulated. The resulting propagation scheme is regarded as a natural extension of the coupled coherent states technique of Shalashilin and Child[24–26] in so far as (i) basis-set elements represent localized quantum states; (ii) each element evolves independently in a generalized classical phase space and carries an action phase; and (iii) the quantum amplitudes associated with individual elements obey fully coupled equations of motion which present a number of attractive qualities.

We begin in §II with an overview on generalized coherent states, deliberately avoiding the underlying group-theoretical formalism associated with their construction. In particular, we demonstrate how the time-dependent variational principle leads to classical equations of motion for the coherent-state parameters in a curved phase space. This preliminary discussion is illustrated with specific examples. Next, in §III, we set forth to derive the working equations of the generalized coupled coherent states method, first in continuum form and then in terms of a discrete basis set. In the latter case, both unitary and non-unitary versions of the formulas are devised. A primitive method, resulting from propagation of a single configuration, is also discussed. In §IV we use our approach to study model Hamiltonians and compare our results against exact quantum data. We also take the opportunity to expose certain particular aspects of the generalized coherent-state formulation. Finally, conclusions are drawn in §V.

II.   GENERALIZED COHERENT-STATE FORMALISM

Coherent states are most elegantly discussed within the context of group theory and this is the point of view adopted here. We shall not venture into the group-theoretical formalism itself though – on that subject the reader is referred to the instructive review by Zhang, Feng and Gilmore[27] or to a recent paper by the present authors.[10] Here, we will rather follow a more pragmatic approach according to which a coherent state is given in the form of an expansion in a proper set of orthonormal states and work its geometrical properties thereon.

A.   Preliminaries

Coherent states are Hilbert space vectors labeled by a complex vector $z = (z_1, \ldots, z_d)$.[28] They can be understood as the result of a Lie-group operator acting on a reference state, which is recovered by setting all entries of the vector z to zero. We shall denote a non-normalized coherent state by $|z\}$. These curly *ket* states are analytical in z, while the *bra* states $\{z|$ are analytical in the complex conjugate variable, denoted by z^*; the normalized state $|z\rangle$ is not analytical in z for it depends on z^* through the normalization factor $\{z|z\}^{-\frac{1}{2}}$. The length d of z will be identified as the number of degrees of freedom of the classical phase space associated with the dynamics of z.

Coherent states of different groups are characterized by their distinct geometrical properties which, in turn, are described in terms of a function f related to the scalar product between two non-normalized coherent states:

$$f(z^*, z') = \log\{z|z'\}. \tag{2.1}$$

The *classical phase-space metric* $g_{\alpha\beta}$ is a hermitian matrix obtained by taking the cross derivatives of the real function $f(z^*, z)$ with respect to its complex arguments, treating z and z^* as independent variables:[29]

$$g_{\alpha\beta}(z^*, z) = \frac{\partial^2 f(z^*, z)}{\partial z_\alpha \partial z_\beta^*}. \tag{2.2}$$

The (non-orthogonal) coherent states span an overcomplete basis of the corresponding Hilbert space and a closure relation holds:

$$\hat{1} = \int d\mu(z^*, z) |z\rangle\langle z|, \tag{2.3}$$

5

where the integration domain depends on the specific type of coherent state being considered – for semisimple compact Lie Groups or the Heisenberg-Weyl group, for example, it extends over the entire d-dimensional complex plane. In (2.3), the *integration measure* $\mathrm{d}\mu(z^*, z)$ is defined as below:

$$\mathrm{d}\mu(z^*, z) = \kappa \det[g(z^*, z)] \prod_{\alpha=1}^{d} \frac{\mathrm{d}^2 z_\alpha}{\pi}, \tag{2.4}$$

where $\mathrm{d}^2 z_\alpha = \mathrm{d}(\mathrm{Re}\, z_\alpha)\mathrm{d}(\mathrm{Im}\, z_\alpha)$ and the constant κ is determined by normalization of (2.3) – e.g. by setting the expectation value of (2.3) in the reference state to unity – and therefore it depends on the quantum numbers that characterize the particular Hilbert space that carries the coherent-state representation (some examples are found below in §II C). In order to shorten the notation, we shall write simply $\mathrm{d}\mu(z)$, but keeping in mind that the measure is a real function of both z and z^*.

B. Classical dynamics

The norm-invariant Lagrangian[30] that gives rise to the Schrödinger equation is

$$L(\psi) = \frac{i\hbar}{2} \left[\frac{\langle\psi|\dot\psi\rangle - \langle\dot\psi|\psi\rangle}{\langle\psi|\psi\rangle} \right] - \frac{\langle\psi|\hat{H}|\psi\rangle}{\langle\psi|\psi\rangle}, \tag{2.5}$$

where $|\psi\rangle = |\psi(t)\rangle$ is an arbitrary quantum state and $\hat{H}$ represents the system's Hamiltonian operator. The time-dependent variational principle (TDVP) states that, given a parametrization of $|\psi\rangle$ in terms of some set of variables, the Euler-Lagrange equations obtained from (2.5) translate into equations of motion for those same variables. If the parametrization is flexible enough an exact quantum solution is achieved. On the other hand, if the parametrization contains less than the number of variables needed to span the associated Hilbert space, the resulting dynamics will be only approximate.

We shall *define* the *classical equations of motion* for z as those equations obtained from the TDVP when a trial state $|\psi\rangle = |z\}$ is substituted in (2.5) – that is, a trial state whose dynamics is restricted to the nonlinear subspace consisting only of coherent states. In this case, equation (2.5) takes the form:

$$L(z) = \frac{i\hbar}{2} \sum_{\alpha=1}^{d} \left[\frac{\partial f(z^*, z)}{\partial z_\alpha} \dot z_\alpha - \frac{\partial f(z^*, z)}{\partial z_\alpha^*} \dot z_\alpha^* \right] - H(z^*, z), \tag{2.6}$$

6

where the *classical Hamiltonian* is the diagonal element of the operator $\hat{H}$ in the coherent-state representation:

$$H(z^*, z) = \frac{\{z|\hat{H}|z\}}{\{z|z\}} = \langle z|\hat{H}|z\rangle. \tag{2.7}$$

By means of the Euler-Lagrange equations one immediately finds that the dynamics of z obeys:

$$\sum_{\beta=1}^{d} \dot{z}_\beta g_{\beta\alpha}(z^*, z) = -\frac{i}{\hbar} \frac{\partial H(z^*, z)}{\partial z_\alpha^*}, \tag{2.8}$$

and that an equivalent (complex conjugate) equation holds for z^*. Notice how the coherent-state geometry introduces a curvature in phase space by means of the metric g. One now can distinguish between two kinds of coupling between the components of the vector z: a *dynamical coupling* via H, and a *geometrical coupling* induced by g.

The group-theoretical formalism assures us that Eq. (2.8) describes a Hamiltonian system in the most strict sense: the phase space exhibits a symplectic structure, since a nondegenerate Poisson bracket can always be established.[27]

Furthermore, the measure (2.4) is invariant under the classical dynamics given by equation (2.8), that is, $d\mu(z(t_2)) = d\mu(z(t_1))$, for any two instants t_1 and t_2 – a property that we recognize as a generalized form of the Liouville theorem and that remains valid even when the system's Hamiltonian has an explicit time dependence.[31]

Finally, we define the *complex action A*:

$$A(z^*(t), z(0), t) = S(z) - \tfrac{i\hbar}{2} \left[f(z^*(t), z(t)) + f(z^*(0), z(0)) \right], \tag{2.9}$$

where the first term is the time integral:

$$S(z) = \int_0^t L(z) \, d\tau, \tag{2.10}$$

with the Lagrangian $L(z)$, given by equation (2.6), being evaluated over a classical orbit, satisfying (2.8).

As can be seen in (2.9), the complex action A carries imaginary surface terms, which ensure that this is a well-defined analytical function on both its complex arguments: $z^*(t)$

and $z(0)$, and also the time t. The derivatives with respect to each of these variables are:

$$\frac{i}{\hbar}\frac{\partial A(z^*(t), z(0), t)}{\partial z^*_\alpha(t)} = \frac{\partial f(z^*(t), z(t))}{\partial z^*_\alpha(t)}, \tag{2.11a}$$

$$\frac{i}{\hbar}\frac{\partial A(z^*(t), z(0), t)}{\partial z_\alpha(0)} = \frac{\partial f(z^*(0), z(0))}{\partial z_\alpha(0)}, \tag{2.11b}$$

$$\frac{\partial A(z^*(t), z(0), t)}{\partial t} = -H(z^*(t), z(t)). \tag{2.11c}$$

The above relations are recognized as the signature of a properly defined classical action integral.[10] Yet it is in terms of the real quantity S of Eq. (2.10) that our results are most conveniently expressed.[34] Therefore we shall denominate S the *action*.

C.   Examples of coherent states

In order to illustrate the formalism presented above, we consider simple examples of coherent states and evaluate some of their geometrical elements, such as the metric matrix g and integration measure $\mathrm{d}\mu$.

1.   *Canonical coherent states*

Canonical coherent states have their functional definition given in terms of a superposition of bosonic Fock states with *unrestricted* occupation numbers; if the Hilbert space comprises n modes, then the non-normalized canonical coherent state is defined by:

$$|z\} = \sum_{m_1=0}^{\infty} \cdots \sum_{m_n=0}^{\infty} \left[\prod_{\alpha=1}^{n} \frac{z_\alpha^{m_\alpha}}{\sqrt{m_\alpha!}}\right] |m_1, \ldots, m_n\rangle, \tag{2.12}$$

where the vacuum $|0, \ldots, 0\rangle$ is the reference state and the length of the vector z equals the number of bosonic modes: $d = n$.

Since the modes are assumed to be orthonormal, it follows immediately from (2.12) that the overlap between canonical coherent states is

$$\{z|z'\} = \exp\left(\sum_{\alpha=1}^{n} z_\alpha^* z'_\alpha\right); \tag{2.13}$$

thus, using (2.1), we identify the function f as:

$$f(z^*, z') = \sum_{\alpha=1}^{n} z_\alpha^* z'_\alpha. \tag{2.14}$$

8

From (2.2), the phase-space metric matrix g is simply the identity matrix:

$$g_{\alpha\beta}(z^*, z) = \delta_{\alpha\beta}, \tag{2.15}$$

which means that canonical coherent states give rise to a flat phase space and therefore the degrees of freedom are not geometrically coupled. The normalized measure, as defined in (2.4), is then trivial:

$$d\mu(z) = \prod_{\alpha=1}^{n} \frac{d^2 z_\alpha}{\pi}. \tag{2.16}$$

In what concerns semiclassical trajectory-based methods, canonical coherent states are undoubtedly the most widely used type of coherent state. This is so because of the following well-known homomorphism connecting the ladder operators $(a_\alpha^\dagger, a_\alpha)$ of each bosonic mode in (2.12) with the position and momentum operators $(\hat{q}_\alpha, \hat{p}_\alpha)$:

$$\hat{q}_\alpha = \frac{\gamma_\alpha}{\sqrt{2}}(a_\alpha^\dagger + a_\alpha), \quad \hat{p}_\alpha = \frac{i\hbar}{\gamma_\alpha\sqrt{2}}(a_\alpha^\dagger - a_\alpha), \tag{2.17}$$

with $[a_\alpha, a_\beta^\dagger] = \delta_{\alpha\beta}$ and where γ_α is an arbitrary constant that sets the appropriate length scale in each mode. The position representation of $|z\rangle$ is then found to be a multidimensional Gaussian wavepacket, whose mean position q and mean momentum p are related to the real and imaginary parts of the complex vector z, respectively. Furthermore, the dynamics of (q, p), as obtained from the time-dependent variational principle, is simply given by Hamilton's classical equations of motion in canonical form, the Hamiltonian being the mean value given by equation (2.7). This so-called 'frozen-Gaussian representation' provides an obviously suitable framework for semiclassical applications.[35–41]

2. SU(n) *bosonic coherent states*

The SU(n) bosonic coherent states are suitable for describing systems in a Fock space comprising n modes and a *fixed* total particle number N. Their non-normalized form is

$$|z\} = \sideset{}{'}\sum_{\{m\}} \left(\frac{N!}{m_1! \ldots m_n!}\right)^{\frac{1}{2}} \left[\prod_{\alpha=1}^{n-1} z_\alpha^{m_\alpha}\right] |m_1, \ldots, m_n\rangle, \tag{2.18}$$

where the reference state is $|0, \ldots, N\rangle$. In (2.18), the primed summation symbol means that the set of occupation numbers $\{m\}$ must satisfy the condition $m_1 + m_2 + \ldots + m_n = N$.

Because of this constraint, the number of entries of the vector z is one less than the number of modes: $d = n - 1$.

The overlap is easily evaluated from (2.18) with the help of the multinomial theorem:

$$\{z|z'\} = \left[1 + \sum_{\alpha=1}^{n-1} z_\alpha^* z_\alpha' \right]^N ;$$ (2.19)

hence, by means of (2.1), all geometrical aspects of these coherent states are codified in the function f given by:

$$f(z^*, z') = N \log \left[1 + \sum_{\alpha=1}^{n-1} z_\alpha^* z_\alpha' \right].$$ (2.20)

The metric matrix, according to (2.2), is:

$$g_{\alpha\beta}(z^*, z) = N \frac{(1 + |z|^2)\delta_{\alpha\beta} - z_\alpha^* z_\beta}{(1 + |z|^2)^2},$$ (2.21)

where $|z|^2 = \sum_{\gamma=1}^{n-1} z_\gamma^* z_\gamma$. Clearly, the fixed particle number condition translates into a geometrical coupling among the components of the vector z.

Despite the complications introduced by the curved geometry, the metric's determinant can be evaluated and the integration measure, defined in (2.4), is found to be:

$$\mathrm{d}\mu(z) = \frac{(N + n - 1)!}{N!(1 + |z|^2)^n} \prod_{\alpha=1}^{n-1} \frac{\mathrm{d}^2 z_\alpha}{\pi}.$$ (2.22)

Recently, semiclassical methods employing $SU(n)$ bosonic coherent states, including an initial value representation based on classical trajectories in a duplicated phase space, have been developed and tested with an $SU(3)$ model Hamiltonian[19,20] – in §IV B we shall have the opportunity to revisit that same problem.

3. Spin coherent states

A particularly interesting $SU(n)$ coherent state originates when the bosonic Fock space has only $n = 2$ modes. The $(N + 1)$ states

$$|N, 0\rangle, |N - 1, 1\rangle, |N - 2, 2\rangle, \ldots, |1, N - 1\rangle, |0, N\rangle$$

can be put into one-to-one correspondence with the well-known simultaneous eigenstates $|J, M\rangle$ of the angular momentum operators $\{\hat{J}^2, \hat{J}_z\}$ for a fixed total angular momentum

10

$J = N/2$. In this way, the non-normalized SU(2) coherent states[27,42] can be expressed as:

$$|z\} = \sum_{M=-J}^{J} \binom{2J}{J+M}^{\frac{1}{2}} z^{J+M} |J, M\rangle, \tag{2.23}$$

which are especially designated as *atomic* or *spin coherent states*. Notice that, in this specific case, the complex vector label z has dimension $d = 1$ and $|J, -J\rangle$ is the reference state.

The overlap $\{z|z'\}$ is easily evaluated using the orthogonality of the $|J, M\rangle$ states. Alternatively, we can simply set $n = 2$ and $N = 2J$ in equation (2.19), thus obtaining:

$$\{z|z'\} = (1 + z^* z')^{2J}, \tag{2.24}$$

which leads to

$$f(z^*, z') = 2J \log(1 + z^* z'). \tag{2.25}$$

According to equation (2.2), it follows that the phase-space metric g (in this case, a scalar) is simply:

$$g(z^*, z) = \frac{2J}{(1 + |z|^2)^2}. \tag{2.26}$$

The normalized measure is then found to be

$$d\mu(z) = \frac{(2J + 1)}{(1 + |z|^2)^2} \frac{d^2 z}{\pi}. \tag{2.27}$$

The natural topology of the spin coherent state is that of the surface of a sphere. In practical applications, one typically writes z in terms of angles θ and ϕ:

$$z = \tan(\theta/2) e^{-i\phi}, \tag{2.28}$$

where $\theta \in [0, \pi]$ and $\phi \in [0, 2\pi)$. In these coordinates the integration measure (2.27) reads:

$$d\mu(\theta, \phi) = (2J + 1) \sin\theta \frac{d\theta d\phi}{4\pi}. \tag{2.29}$$

Spin coherent states are discussed in more detail in §IV A where we investigate a test model consisting of an SU(2) Hamiltonian.

4. SU(n) *fermionic coherent states*

Fermionic coherent states of the special unitary group are suitable for describing a number-conserving system of N fermions which are allowed to occupy a set of n orthonormal

11

single-particle states ($n > N$). While ultimately arbitrary, these underlying single-particle states are often taken to be eigenstates of the non-interacting part of the Hamiltonian or a set of Hartree-Fock spin orbitals.[13,27] A reference state $|\Phi_0\rangle$ is specified by constructing a Slater determinant out of N of such spin orbitals (e.g. the ones having lowest energies). These are denoted by $|\phi_\alpha^\bullet\rangle$ with $1 \leq \alpha \leq N$, and are said to belong to the *occupied* space. The remaining $M \equiv n - N$ spin orbitals, denoted by $|\phi_\mu^\circ\rangle$ with $1 \leq \mu \leq M$, are said to belong to the *virtual* space. Then, the non-normalized fermionic coherent state can written as:

$$|z\} = \hat{A}_N \prod_{\alpha=1}^{N} \left[|\phi_\alpha^\bullet\rangle + \sum_{\mu=1}^{M} |\phi_\mu^\circ\rangle z_{\mu\alpha} \right], \tag{2.30}$$

where the symbol $\hat{A}_N$ instructs anti-symmetrization of the direct product of the N single-particle states $|\phi_\alpha^\bullet\rangle + \sum_{\mu=1}^{M} |\phi_\mu^\circ\rangle z_{\mu\alpha}$, which are sometimes called *dynamical orbitals*.[15]

In the context of quantum chemistry the coherent state (2.30) is designated as the *Thouless parametrization* of a Slater determinant.[12] Here, the label z is understood as an $M \times N$ matrix, the number of degrees of freedom of the corresponding phase space being $d = M \times N$. The elements $z_{\mu\alpha}$ describe the mixing between occupied and virtual spin orbitals in such a way that any single-determinantal state not orthogonal to $|\Phi_0\rangle = \hat{A}_N \prod_{\alpha=1}^{N} |\phi_\alpha^\bullet\rangle$ can be represented by $|z\}$.[44]

The overlap between two distinct Thouless-parametrized Slater determinants is readily found to be:

$$\{z|z'\} = \det(I_N + z^\dagger z'), \tag{2.31}$$

where I_N is the identity matrix of size $N \times N$. Following the definitions given in §II, geometrical properties are determined from the function:

$$f(z^*, z') = \log[\det(I_N + z^\dagger z')]. \tag{2.32}$$

From (2.2), one finds (through elementary determinant and matrix identities) that the phase-space metric can be expressed as:

$$g_{\mu\nu,\alpha\beta}(z^*, z) = [(I_M + zz^\dagger)^{-1}]_{\nu\mu}[(I_N + z^\dagger z)^{-1}]_{\alpha\beta}, \tag{2.33}$$

where I_M is the $M \times M$ identity matrix and the derivatives of f were taken with respect to $z_{\mu\alpha}$ and $z_{\nu\beta}^*$. Despite the complicated outlook of (2.33) the classical equations of motion for the Thouless parameters z, as governed by a standard many-body Hamiltonian consisting

of one- and two-body terms, display a simple structure – see, for instance, Section IIIA in Ref. 15.

Finally, the integration measure appearing in the closure relation (2.3) is found to be:

$$\mathrm{d}\mu(z^*, z) = \kappa \left[\det(I_N + z^\dagger z) \right]^{-n} \prod_{\alpha=1}^{N} \prod_{\mu=1}^{M} \frac{\mathrm{d}^2 z_{\mu\alpha}}{\pi}. \tag{2.34}$$

The normalization constant can be computed by evaluating the required phase-space integral through a recurrence relation method; the result is $\kappa = \prod_{\gamma=1}^{N} \frac{(n+1-\gamma)!}{(N+1-\gamma)!}$.

As one might infer from the above, fermionic coherent states of this kind are somewhat more intricate than the ones discussed in the previous examples. And, although the content of the present paper encompasses all basic ingredients needed to implement the proposed method in terms of these states, a proper treatment would nevertheless require introduction of additional concepts. Therefore, we do not pursue applications involving this particular set of coherent states in this paper.

III. GENERALIZED CCS METHOD

The coupled coherent states (CCS) method, as originally developed by Shalashilin and Child[24–26] using canonical coherent states, belongs to the family of multiconfigurational guided-basis methods. Its characteristic attributes are the non-orthogonality of the basis set and the use of simple classical mechanics[43] to guide the basis elements, as opposed to more complicated full-variational approaches like the Gaussian-based version of the multiconfigurational time-dependent Hartree (G-MCTDH) method.[45–47]

Formulation of the method for Gaussian states is fairly straightforward and the same is true in the generalized context. In order to better appreciate the additional features that arise in the latter case, we will first present the method in its continuum form; the discrete version is developed subsequently.

A. The continuum version

We begin by considering the coherent-state decomposition of an arbitrary quantum state,

$$|\psi\rangle = \int \mathrm{d}\mu(z)|z\rangle\langle z|\psi\rangle = \int \mathrm{d}\mu(z_0)|z\rangle\langle z|\psi\rangle, \tag{3.1}$$

which follows from (2.3). It is assumed that $z = z(t)$ is bound to obey the classical equations of motion (2.8). By virtue of phase-space volume conservation, we are allowed to transfer the integration measure to the initial instant and conveniently integrate over initial conditions $z_0 = z(0)$, as indicated in the second equality in (3.1). The derivation of the CCS equations amounts to finding a solution of the Schrödinger equation

$$i\hbar|\dot{\psi}\rangle = \hat{H}|\psi\rangle, \tag{3.2}$$

for $|\psi\rangle$ in the form given by (3.1) with the *ansatz*:

$$\langle z|\psi\rangle = C(z)e^{\frac{i}{\hbar}S(z)}, \tag{3.3}$$

where $S(z)$ is the action defined in (2.10). In other words, we seek an equation of motion for the time-dependent amplitude $C(z)$ that solves (3.2). Let us make a few observations regarding this particular choice of solution.

First, all quantities that specify $|\psi\rangle$ – i.e. $|z\rangle$, $C(z)$ and $S(z)$ – are to be regarded as functions of the initial conditions z_0. Thus, the method is conceived as an initial value representation from its onset.

Second, we note that it follows from (3.3) that $C(z)$ depends on the initial state $|\psi_0\rangle = |\psi(0)\rangle$ through the relation $C(z_0) = \langle z_0|\psi_0\rangle$. In numerical applications, the integral in (3.1) has to be approximated somehow; the typical procedure is to sample initial conditions z_0 in phase space with the overlap modulus $|\langle z_0|\psi_0\rangle|$ playing the role of a weight function. Once the z_0's have been properly sampled, the values of the corresponding $C(z_0)$'s are uniquely defined.

Third, the motivation behind the factorization of $\langle z|\psi\rangle$ into a complex amplitude times an action exponential comes from a general result of semiclassical theory, according to which the classical action provides a first-order approximation to the phase of the quantum state. Since this phase accounts for most of the wavefunction's oscillatory behavior, $C(z)$ is expected to present a rather smooth time dependence, thus facilitating numerical treatment.

We now proceed to look for a differential equation for $C(z)$. Taking the time derivative of (3.3) and making use of the Schrödinger equation, we find (after rearranging terms):

$$i\hbar \dot{C}(z) = \left[i\hbar\langle\dot{z}|\psi\rangle + \langle z|\hat{H}|\psi\rangle + L(z)\langle z|\psi\rangle\right]e^{-\frac{i}{\hbar}S(z)}. \tag{3.4}$$

Next, we factor out $|\psi\rangle$ by separating the scalar products on the right-hand side of the equation with the help of the closure relation $\hat{1} = \int d\mu(z')|z'\rangle\langle z'|$, with $z' = z'(t)$, which

leads to

$$i\hbar\,\dot{C}(z) = \int \mathrm{d}\mu(z_0')\langle z|z'\rangle \Delta^2 H(z^*,z')C(z')e^{\frac{i}{\hbar}[S(z')-S(z)]}. \tag{3.5}$$

Here we have already shifted the integration measure to the initial instant $[z_0' = z'(0)]$ and replaced the $\langle z'|\psi\rangle$ that appeared under the integral sign for $C(z')e^{\frac{i}{\hbar}S(z')}$.

The coupling $\Delta^2 H(z^*,z')$ in (3.5) is given by

$$\Delta^2 H(z^*,z') = i\hbar\frac{\langle \dot{z}|z'\rangle}{\langle z|z'\rangle} + H(z^*,z') + L(z), \tag{3.6}$$

where the non-diagonal matrix element

$$H(z^*,z') = \frac{\{z|\hat{H}|z'\}}{\{z|z'\}} = \frac{\langle z|\hat{H}|z'\rangle}{\langle z|z'\rangle}, \tag{3.7}$$

is an analytical function of z^* and z' that can be directly obtained by analytical continuation of the classical Hamiltonian (2.7).

As a last step, we express the first term in (3.6) as a function of readily computable quantities. Since $\langle z| = e^{-\frac{1}{2}f(z^*,z)}\{z|$ we observe that:

$$\frac{\langle \dot{z}|z'\rangle}{\langle z|z'\rangle} = \frac{\{\dot{z}|z'\}}{\{z|z'\}} - \frac{1}{2}\frac{\mathrm{d}}{\mathrm{d}t}f(z^*,z).$$

The total time derivative of $f(z^*,z)$ is simply

$$\frac{\mathrm{d}}{\mathrm{d}t}f(z^*,z) = \sum_{\alpha=1}^{d}\left[\frac{\partial f(z^*,z)}{\partial z_\alpha^*}\dot{z}_\alpha^* + \frac{\partial f(z^*,z)}{\partial z_\alpha}\dot{z}_\alpha\right],$$

while the remaining term involving $\{\dot{z}|$ can be written as

$$\frac{\{\dot{z}|z'\}}{\{z|z'\}} = \sum_{\alpha=1}^{d}\frac{\partial f(z^*,z')}{\partial z_\alpha^*}\dot{z}_\alpha^*,$$

owing to the the analyticity of $\{z|$ on z^*. Hence, collecting together the above results and making the necessary substitutions in (3.6), we find that the coupling may be expressed as:

$$\Delta^2 H(z^*,z') = H(z^*,z') - H(z^*,z) + i\hbar\sum_{\alpha=1}^{d}\left[\frac{\partial f(z^*,z')}{\partial z_\alpha^*} - \frac{\partial f(z^*,z)}{\partial z_\alpha^*}\right]\dot{z}_\alpha^*; \tag{3.8}$$

which is an analytic function on z'.

By integrating the equation of motion (3.5) the amplitudes at time t can be determined from their initial values. Once the amplitudes are known, we can reconstruct the quantum state with (3.1), reproduced below in terms of $C(z)$:

$$|\psi\rangle = \int \mathrm{d}\mu(z_0)|z\rangle C(z)e^{\frac{i}{\hbar}S(z)}. \tag{3.9}$$

The integro-differential equation (3.5) – with $\Delta^2 H(z^*, z')$ given by (3.8) – relates directly to the canonical coherent states version of the CCS method and shares its attractive characteristics, namely: (i) in the semiclassical regime, according to the reasons mentioned earlier, the amplitude $C(z)$ is expected to have a smooth time dependence; (ii) because of the coherent-state overlap $\langle z|z' \rangle$, the z' integral is localized around z;[48] and (iii) the coupling between amplitudes of different basis elements is not only sparse but also non-diagonal, since the integrand is identically zero when $z' = z$.

As a final remark, we should note that, if one performs a series expansion of $\Delta^2 H(z^*, z')$ for small $|z'-z|$, one finds that this series begins with a second-order term. In the generalized coherent state case however, unlike the specific situation for canonical coherent states, this does not coincide with the second- and higher-order terms in the Taylor series of $H(z^*, z')$.

B.   The discrete version

Here we re-derive the CCS equations using a discrete set of coherent states as basis, as opposed to the continuous set employed in the previous section. We shall find that the discrete formulas do not differ from their analogue expressions in the canonical coherent state case. This is due to the fact that all information concerning distinct coherent-state geometries is codified in a number of key quantities, namely: the overlap, the phase-space metric and the classical equations of motion. Each of these quantities participates in the same way in the working equations, regardless of the particular type of coherent state being used – incidentally, a most desirable feature for programming purposes, for it means that the core subroutines of the method are essentially independent of geometry. Nevertheless, for the sake of consistency, we must review the discrete formulas, for they are the ones actually used in practice.

1.   Unitary propagation

The first step towards a discrete unitary formulation of the generalized CCS method is the assumption that one is able to write down a closure relation by employing a finite

number of basis elements as below:

$$\hat{1} = \sum_{j=1}^{M} \sum_{k=1}^{M} |z_j\rangle \Lambda_{jk} \langle z_k|, \tag{3.10}$$

where M is the size of the basis set.[49] It suffices that this closure relation represents the identity operator only on the dynamically accessible part of the phase space and that it holds only during the time interval upon which the propagation takes place.

In order to properly represent the identity, the matrix Λ in (3.10) must satisfy the relation:

$$\delta_{jk} = \sum_{l} \Omega_{jl} \Lambda_{lk}, \tag{3.11}$$

where

$$\Omega_{jk} = \langle z_j | z_k \rangle, \tag{3.12}$$

is the *overlap matrix*. This guarantees that we have a well-defined discrete coherent-state decomposition:

$$|\psi\rangle = \sum_{j,k} |z_j\rangle \Lambda_{jk} \langle z_k | \psi \rangle. \tag{3.13}$$

In other words, Ω must be sufficiently well-conditioned so that expressions involving its inverse Λ remain numerically stable during the entire propagation. Therefore, the basis-set initial conditions must be sampled in such a way as to ensure that this requirement is fulfilled. One such procedure, that results in a well-conditioned overlap matrix (at initial time), is described in appendix A.

Yet, nothing prevents that an initially well-conditioned overlap matrix becomes singular at some later time – a notable weakness of time-dependent methods formulated with non-orthogonal basis sets.[50] In the event that Ω becomes singular, one should take appropriate measures before resuming the propagation. In this regard, a particularly interesting protocol has been proposed by Habershon.[51] The 'singularity problem', though, did not occur in the simple applications considered in this paper.

Upon these considerations, we introduce a discrete set of M amplitudes $C_j = C(z_j)$ as well as their corresponding action phases $S_j = S(z_j)$, writing:

$$\langle z_j | \psi \rangle = C_j e^{\frac{i}{\hbar} S_j}. \tag{3.14}$$

Next, we proceed exactly as in §III A. The equation of motion in the discrete unitary case

is then readily found to be:

$$i\hbar \, \dot{C}_j = \sum_{k,l} \Omega_{jk} \, \Delta^2 H_{jk} \, \Lambda_{kl} \, C_l \, e^{\frac{i}{\hbar}(S_l - S_j)}, \tag{3.15}$$

with coupling matrix given by:

$$\Delta^2 H_{jk} = H(z_j^*, z_k) - H(z_j^*, z_j) + i\hbar \sum_{\alpha=1}^{d} \left[\frac{\partial f(z_j^*, z_k)}{\partial z_{j\alpha}^*} - \frac{\partial f(z_j^*, z_j)}{\partial z_{j\alpha}^*} \right] \dot{z}_{j\alpha}^*. \tag{3.16}$$

In practice matrix Λ is never explicitly constructed; rather, one introduces a set of auxiliary amplitudes $D = (D_1, D_2, \ldots, D_M)$ which are related to the coefficients $C = (C_1, C_2, \ldots, C_M)$ according to

$$\sum_k \Omega_{lk} D_k e^{\frac{i}{\hbar}(S_k - S_l)} = C_l. \tag{3.17}$$

Thus, at every time step D is obtained from C by means of the above intermediate equation – an operation that requires solving a linear system of size M. Then, the equation of motion (3.15) can be recast as:

$$i\hbar \, \dot{C}_j = \sum_k \left[\Omega_{jk} \, \Delta^2 H_{jk} \, e^{\frac{i}{\hbar}(S_k - S_j)} \right] D_k, \tag{3.18}$$

while the quantum state is expressed in terms of amplitudes D as:

$$|\psi\rangle = \sum_k |z_k\rangle D_k e^{\frac{i}{\hbar}S_k}. \tag{3.19}$$

The propagation scheme comprised by Eqs. (2.8), (3.17), (3.18), and (3.19) represents the standard form of the generalized coherent-state method proposed here. It can be shown to preserve normalization – given by the sum $\sum_k C_k^* D_k$ – as long as the overlap matrix remains sufficiently well-conditioned. In addition, it preserves total energy (for time-independent Hamiltonians) as long as the identity operator can be resolved in terms of the basis-set elements, though this situation is hardly achieved in multidimensional problems. It has been pointed out that energy conservation is closely related to the accuracy of the CCS method.[51] Thus, by monitoring total energy, one can make an 'on-the-fly' diagnosis as regards to the quality of the CCS results; indeed we observe in our simulations that deviations from the exact quantum solution are accompanied by fluctuations in total energy.

2. Non-unitary case

It may be convenient – particularly when the system under study has only one or two degrees of freedom – to attempt a more straightforward discretization of the closure relation, as below:

$$\hat{1} \approx \sum_{k=1}^{M} |z_k\rangle \lambda_k \langle z_k|, \tag{3.20}$$

with λ_k approximating the integration measure $\mathrm{d}\mu(z_k)$ at each phase-space point.

The equation of motion for C in this case can be obtained at once from (3.15) by setting $\Lambda_{kl} = \lambda_k \delta_{kl}$:

$$i\hbar\,\dot{C}_j = \sum_k \lambda_k \left[\Omega_{jk}\,\Delta^2 H_{jk}\,e^{\frac{i}{\hbar}(S_k - S_j)} \right] C_k. \tag{3.21}$$

Similarly, the quantum state in this case is given by:

$$|\psi\rangle = \sum_k \lambda_k |z_k\rangle C_k e^{\frac{i}{\hbar}S_k}. \tag{3.22}$$

This propagation scheme is computationally less demanding than the one discussed in the previous section – if the basis-set size is kept the same –, since there is no need to solve a linear system at each time step. On the other hand, a larger basis set (usually constructed as a grid in phase space) may be necessary to converge the results if (3.21) is employed. Moreover, as discussed by Shalashilin and Child,[26] the direct discretization of equation (3.5) does not preserve the unitarity of an exact quantum time evolution, that is, the norm of the propagated quantum state is not automatically conserved, meaning that results must be normalized on output.

C. Classical propagation

To end this section, we discuss the particular situation whereupon a single coherent-state basis element is used to describe the system:

$$|\psi\rangle = |z\rangle e^{\frac{i}{\hbar}S(z)}. \tag{3.23}$$

As can be seen from the above equation, this scheme only applies if the quantum state to be propagated is a coherent state, that is: $|\psi_0\rangle = |z_0\rangle$. The form of the approximated $|\psi\rangle$, with an action phase, can be derived from the working equations of the previous sections by setting the basis-set size $M = 1$, in which case we find that $\dot{C} = 0$ and hence $C(t) = C(0) = 1$.

We shall denominate the primitive method defined by (3.23), together with (2.8) and (2.10), as the *classical propagation scheme*, in view of the fact that only classical ingredients are present in its formulation. It serves as a reference method, against which more sophisticated approaches, such as those described earlier, may be confronted – which is useful, for example, in order to identify non-classical behavior (defined in this sense), as in §IV B.

It should be pointed out that if the Hamiltonian of the system is such that application of the time-evolution operator maps one coherent state onto another – or, more formally, when the Hamiltonian is an element of the Lie algebra associated with the set of coherent states under consideration –, then the classical propagation scheme actually gives the exact solution. In other situations it may provide a reasonable approximation for very short times.

IV.   APPLICATION EXAMPLES

A.   Condensate in a double-well potential

As a first application we consider a simplified model for the dynamics of an N-particle Bose-Einstein condensate trapped in a double-well potential, where individual bosons interact through contact forces, that is, with an interacting potential $V(\mathbf{x}, \mathbf{x}') \propto \delta(\mathbf{x} - \mathbf{x}')$. This model has been discussed in detail in several works;[52–54] here we briefly sketch its main ideas.

In the two-mode approximation, it is assumed that only the single-particle ground state and first excited state of the double-well potential, as obtained from first-order perturbation theory, have a significant occupation, so that the dynamics of the system is restricted to these two levels. This should be a good approximation if one seeks to describe the low temperature regime, wherein most of the particles are expected to be occupying the ground state – see Ref. 55 for a discussion on the validity of the two-mode approximation to the double-well problem.

Since the number of bosons is preserved, the particle number operator $\hat{N}$ is a constant of the motion. By means of a well-known homomorphism between the algebra su(2) and the bosonic creation and annihilation operators, the bosonic dynamics can be described in terms of three independent angular momentum operators – Schwinger's pseudo-spin operators[56] – with total angular momentum $J = N/2$.

In terms of these operators the Hamiltonian of the model is:[57]

$$\hat{H} = \Omega \hat{J}_x + \frac{2\chi}{N-1}\hat{J}_z^2, \tag{4.1}$$

where the tunneling rate Ω equals the energy difference between the two occupied single-particle states and the self-collision parameter χ is proportional to the interaction strength of bosons located in the same potential well.

Applying definitions (2.7) and (2.23) to (4.1), the classical Hamiltonian becomes[58]

$$H(z^*, z) = \frac{N\Omega}{2}\frac{z+z^*}{1+z^*z} + \frac{N\chi}{2}\frac{(1-z^*z)^2}{(1+z^*z)^2}, \tag{4.2}$$

in which we discarded, without any loss, a constant term. From identity (2.8), the equation of motion for $z(t)$ is:

$$i\dot{z} = \frac{\Omega}{2}(1-z^2) + 2\chi\frac{z(z^*z-1)}{1+z^*z}. \tag{4.3}$$

Notice that the $(N-1)^{-1}$ scaling of the self-collision parameter in (4.1) was specifically chosen so that the equation of motion (4.3) is independent of particle number N, therefore representing a well-defined classical limit of the system when $N \to \infty$. This also means that, by employing the CCS method with a fixed set of classical trajectories, we can obtain quantum solutions for different particle number regimes.

1. Non-unitary CCS with spin coherent states

We shall examine the quantum dynamics of the Hamiltonian (4.1) from the perspective of a non-unitary implementation of the CCS method. Following the procedure outlined in §III B 2, a direct discretization of expressions (3.5) and (3.9) is performed by replacing the integrals over phase-space variables at $t = 0$ by finite summations over a discrete set of initial conditions.

The accuracy of this straightforward discretization procedure is strongly dependent on the selection of initial values over the phase space. In the particular case of a regular grid, results are found to be extremely sensitive to characteristics such as spacing, placement, number of points and, most importantly, the choice of grid variables.

For the subsequent numerical calculations, we consider a regular grid in the phase-space coordinates (η, ζ), which are related to the SU(2) angular coordinates (θ, ϕ) defined in equa-

tion (2.28), according to:

$$\eta = \theta, \tag{4.4}$$

$$\zeta = \phi \sin \theta. \tag{4.5}$$

This choice aims at reducing the inherent difficulties imposed by the spherical topology of spin coherent states at $\theta \approx 0$ or π.

In terms of this new set of coordinates, the integration measure (2.29) takes a simpler form:

$$d\mu = \frac{2J+1}{4\pi} d\eta d\zeta, \tag{4.6}$$

which, unlike expressions (2.27) and (2.29), is independent of the integration variables. Hence, the λ_k's that appear in the non-unitary evolution equation (3.21) and also in (3.22) are all equal to the same time-independent λ given by:

$$\lambda = \frac{2J+1}{4\pi} \Delta\eta\Delta\zeta, \tag{4.7}$$

where $\Delta\eta$ and $\Delta\zeta$ are the grid spacings in the η and ζ directions, respectively.

The initial quantum state to be propagated is chosen to be the spin coherent state $|\psi_0\rangle = |z'\rangle$ with

$$z' = \tan(\pi/8),$$

specified by angular coordinates $(\theta', \phi') = (\frac{\pi}{4}, 0)$. As it is usually assumed in most guided-basis methods, the most important dynamical contributions – at least for short-time propagation – are expected to arise from classical trajectories initially located at the same phase-space region occupied by $|\psi_0\rangle$. Therefore, the grid of initial conditions is intentionally centered at the point (θ', ϕ'), as illustrated on the left panel of Fig. 1 for the particular case of $N = 100$ particles – the right panel portrays the classical dynamics in phase space. Notice that the classical trajectory with initial value z' is located close to a stable equilibrium point and within the boundaries of a separatrix of motion.

With the purpose of quantifying the agreement between the CCS-propagated quantum state $|\psi_{ccs}(t)\rangle$ and the exact result $|\psi_{exact}(t)\rangle$ – obtained via diagonalization of (4.1) in the angular momentum basis – we shall compute the *fidelity*:

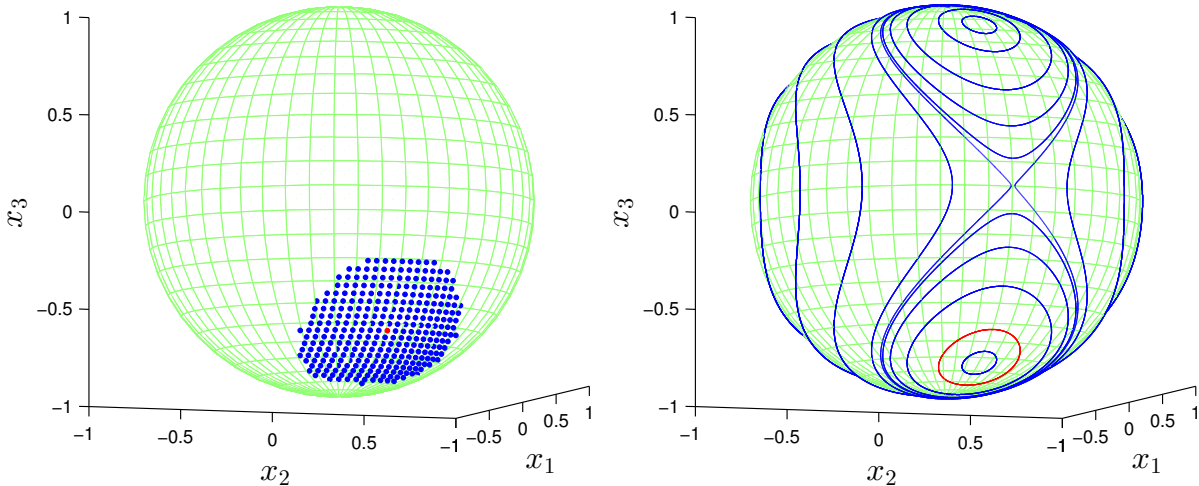$$\mathcal{F}(t) = |\langle \psi_{exact}(t)|\psi_{ccs}(t)\rangle|. \tag{4.8}$$

FIG. 1. Left panel: regular grid of classical initial conditions with approximately three hundred initial values for the case of $N = 100$ particles. The red dot indicates the center of the grid, whose angular coordinates are $(\theta', \phi') = (\frac{\pi}{4}, 0)$. This phase-space point represents the label of the initial coherent state $|\psi_0\rangle = |z'\rangle$. Right panel: some examples of classical trajectories over the spherical phase space. The red orbit corresponds to the initial value z'. The Cartesian coordinates used to plot these trajectories are related to the coherent-state angular variables according to $(x_1, x_2, x_3) = (\sin\theta\cos\phi, \sin\theta\sin\phi, -\cos\theta)$.

The fidelity reflects the physical similarity between two states: its values are restricted to the interval $0 \leq \mathcal{F} \leq 1$, with the maximum value corresponding to physically identical quantum states.

We wish to analyze the behavior of $\mathcal{F}(t)$ as the number of particles in the system is changed. There is a subtlety involved, though: due to its fundamental property of minimal uncertainty,[59,60] the coherent state $|z\rangle$ represents a quantum state with maximal localization in phase space around the point z. Moreover, for spin coherent states, the linear dimensions of the phase-space region effectively occupied by $|z\rangle$ decrease proportionally to $1/\sqrt{N}$.[61] Thus, in order to make a meaningful comparison amongst trajectory-based propagations carried out at different particle number regimes, one must account for the 'shrinking' of the initial state $|\psi_0\rangle = |z'\rangle$ as N grows larger. Therefore, in our simulations, the grid spacing was reduced proportionally to $1/\sqrt{N}$ whilst the number of initial conditions in each run was roughly unchanged.
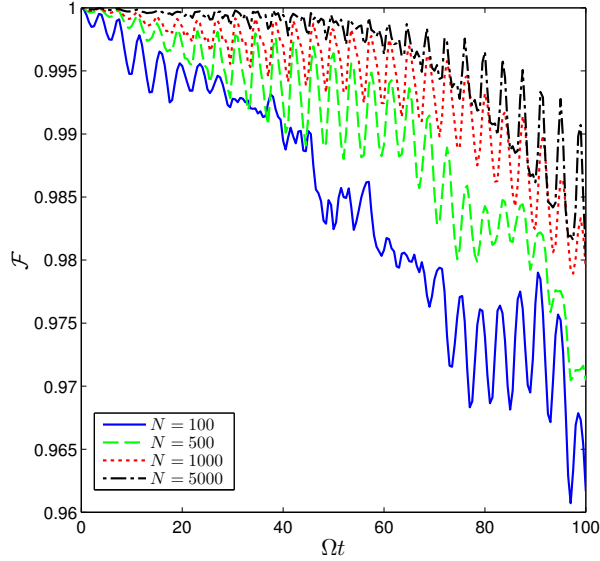
FIG. 2.   Fidelity as a function of the dimensionless time Ωt with parameters $\Omega = 1.0$, $\chi = 1.0$ for different particle number regimes. Each run employed roughly three hundred trajectories – the number of points varies slightly for different runs due to the cropping of grid borders.

Fig. 2 shows $\mathcal{F}$ as a function of time for various values of N. Notice that, even for long times, the non-unitary results remain accurate ($\mathcal{F} > 0.96$). On the other hand, it is clear that the fidelity tends to decrease over time, evidencing the accumulation of numerical errors in the CCS dynamics. In part, this inaccuracy stems from the non-unitary nature of the discretization procedure. However, to a large extent, numerical error arises due to dispersion of the classical trajectories over phase space, resulting in an incomplete description of the quantum system.

Also note that the fidelity is consistently higher for larger particle numbers. Since the number of classical trajectories was kept nearly constant for all the runs, and the range of the initial condition grid was adjusted so as to reflect the width of the initial quantum state, we may conclude that the CCS method is better suited for describing the dynamics in the *many-particle regime*, which we recognize as the *semiclassical regime* for this problem. Indeed, it is well known that the limiting case $N \to \infty$ (or $J \to \infty$, as it can be interpreted in this problem) coincides with the classical limit of quantum mechanics.[62]

In this sense, the CCS method, though in principle formulated as an exact method, when numerically implemented – and therefore subjected to inevitable practical limitations

– should be regarded more as a semiclassical technique than a genuine quantum approach, an assertion that can be made with respect to both its non-unitary and unitary versions.

Finally, we point out that, for the system under consideration, the computational cost of the method is insensitive to particle number. Hence, for very large values of N, the computational resources needed for evaluating the exact quantum dynamics by diagonalization of the Hamiltonian (4.1) will certainly exceed the analogous requirements of the non-unitary CCS method.

B. Condensate in a triple-well potential

Next, we consider a simplified model describing an N-particle Bose-Einstein condensate trapped in a symmetric triple-well potential where individual bosons are once more assumed to interact by contact forces; the main ideas involved are as follows: the triple-well trapping potential, under suitable conditions, can be approximated by an harmonic expansion around each of its three (symmetrically located) minima. The three-fold degenerate fundamental states of this approximated problem can be determined without difficulty. It is then assumed that the dynamical regime is such that the energy eigenspace spanned by these three local modes is sufficiently isolated from the rest of the single-particle spectra, so that at low temperatures they alone provide an adequate description of the system. For more details on the derivation and particularities of this model, see Refs. 63 and 64.

Let a_1, a_2 and a_3 denote the annihilation operators associated with the aforementioned fundamental single-particle modes related to the locally approximated wells. In terms of these bosonic operators, the 'three-mode approximation'[64] to the Hamiltonian is:

$$\hat{H} = \Omega \sum_{1 \leq \alpha \neq \beta \leq 3} a_\alpha^\dagger a_\beta + \frac{\chi}{N-1} \sum_{1 \leq \gamma \leq 3} a_\gamma^\dagger a_\gamma^\dagger a_\gamma a_\gamma, \tag{4.9}$$

where Ω is the tunneling rate, describing hops between adjacent wells, and χ is the collision parameter, that controls the strength of two-body interactions within the same well.[65]

Owing to particle number conservation, this system is suitably described in terms of SU(3) bosonic coherent states $|z\rangle = |z_1, z_2\rangle$, which represent a particular case of the coherent states discussed in §II C 2. Using definition (2.18) together with (4.9), we find from (2.7) that the classical Hamiltonian is

$$H(z^*, z) = N\Omega \frac{(z_1^* z_2 + z_2^* z_1 + z_1^* + z_1 + z_2^* + z_2)}{1 + z_1^* z_1 + z_2^* z_2} + N\chi \frac{(z_1^* z_1)^2 + (z_2^* z_2)^2 + 1}{(1 + z_1^* z_1 + z_2^* z_2)^2}. \tag{4.10}$$

From (2.8) it follows that the equations of motion are:

$$i\dot{z}_1 = \Omega(1 + z_1 + z_2)(1 - z_1) - \frac{2\chi z_1(1 - |z_1|^2)}{1 + |z_1|^2 + |z_2|^2}, \tag{4.11a}$$

$$i\dot{z}_2 = \Omega(1 + z_1 + z_2)(1 - z_2) - \frac{2\chi z_2(1 - |z_2|^2)}{1 + |z_1|^2 + |z_2|^2}. \tag{4.11b}$$

Similarly to the double-well model, we have deliberately tuned the collision parameter χ with a $(N-1)^{-1}$ factor, thereby making the classical dynamics independent of particle number; in this way the classical system is well-defined in the limit $N \to \infty$.

1. *Unitary CCS with* SU(3) *bosonic coherent states*

The classical system defined in (4.11) has three dynamically equivalent invariant subspaces, specified by the constraints: $z_1 = z_2$, $z_1 = 1$ and $z_2 = 1$. Let us concentrate on the first of these ($z_1 = z_2$) and refer to it as the Γ_1 subspace.

Now, consider the set of operators b_1, b_2 and b_3, defined by the canonical transformation:

$$b_1 = \tfrac{1}{\sqrt{2}}(a_1 + a_2), \tag{4.12a}$$

$$b_2 = a_3, \tag{4.12b}$$

$$b_3 = \tfrac{1}{\sqrt{2}}(a_1 - a_2). \tag{4.12c}$$

It can be demonstrated that Γ_1 is an SU(2) subspace whose two single-particle modes are associated with operators b_1 and b_2.[64] As a consequence, under the *classical approximation* described in §III C, any SU(3) coherent state initially located in Γ_1 will always display zero occupation of the b_3 mode; as a matter of fact, the expectation value

$$\langle z | b_3^\dagger b_3 | z \rangle = \frac{N}{2} \frac{(z_1^* - z_2^*)(z_1 - z_2)}{1 + z_1^* z_1 + z_2^* z_2}, \tag{4.13}$$

is identically null when $z_1 = z_2$.

This conclusion, however, does not apply for the actual quantum problem: even if the initial state $|\psi_0\rangle$ has null occupation in the b_3 mode, this situation will not be preserved as the system evolves in time. It is precisely this 'non-classical behavior' that we wish to describe using the SU(3) CCS method.

Let us then consider the following initial state $|\psi_0\rangle = |z_1', z_2'\rangle$, with

$$z_1' = z_2' = \tfrac{1}{\sqrt{2}} \tan(\pi/8),$$

and thus located on the classical invariant subspace Γ_1. We shall propagate this state employing the unitary method developed in §III B 1 and compute the occupation $Q(t) = \langle\psi(t)|b_3^\dagger b_3|\psi(t)\rangle$ of the single-particle mode associated with b_3. Following (3.19), this function will be calculated according to:

$$Q = \sum_{j,k} D_j^* D_k \Omega_{jk} \left[\frac{\{z_j|b_3^\dagger b_3|z_k\}}{\{z_j|z_k\}} \right] e^{i(S_k - S_j)}, \tag{4.14}$$

where the non-diagonal matrix elements between square brackets can be obtained by analytic continuation of (4.13). We shall also monitor the total energy of the system,

$$E = \sum_{j,k} D_j^* D_k \Omega_{jk} H(z_j^*, z_k) e^{i(S_k - S_j)}, \tag{4.15}$$

as a means to probe the quality of our results.

In order to construct the basis set, it is necessary to choose adequate sampling variables. In the present case we opt for angular variables $(\theta_1, \phi_1, \theta_2, \phi_2)$ defined by:

$$z_1 = \tan(\theta_1/2)e^{-i\phi_1}, \tag{4.16}$$

$$z_2 = \tan(\theta_2/2)e^{-i\phi_2}. \tag{4.17}$$

The initial conditions $z(0)$ are then randomly sampled around $z' = (z_1', z_2')$ from Gaussian probability distributions expressed in terms of these angular variables, with each angle being individually selected: for example, $\theta_1(0)$ and $\phi_1(0)$ are selected according to

$$\sim e^{-[\theta_1(0) - \theta_1']^2/2\sigma_{\theta_1}}; \ \sim e^{-[\phi_1(0) - \phi_1']^2/2\sigma_{\phi_1}}. \tag{4.18}$$

Notice that the widths of these distributions are adjustable parameters of the method. The actual sampling procedure – which also comprises specific criteria for accepting and neglecting candidate basis elements – is somewhat involved and further details are reserved to appendix A. Once the basis-set initial conditions are known, the amplitudes C and D of Eqs. (3.14) and (3.17) can be initialized and propagation of (3.18) may be started.

We studied the case of $N = 100$ trapped bosons, with tunneling rate $\Omega = -1.0$, and collision parameter $\chi = -1.0$. The widths of the Gaussian distributions – exemplified in (4.18) – were set to $\frac{\pi}{20}$ for both θ_1 and θ_2 and to $\frac{\pi}{10}$ for both ϕ_1 and ϕ_2.

In order to visualize whether results converge as the basis-set size M is increased, simulations have been performed with different number of orbits while maintaining all other parameters – including sampling widths and random number generator seed[66] – fixed.
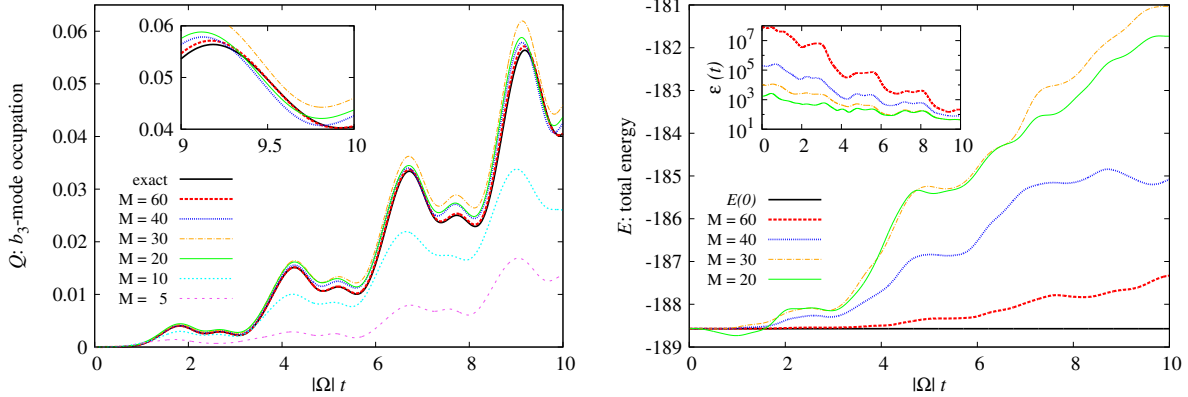
FIG. 3. Left panel: Occupation of the classically inaccessible b_3 mode as a function of dimensionless time $|\Omega|t$ for $N = 100$, $\Omega = -1.0$, and $\chi = -1.0$ and different basis-set sizes M; inset: zoom on the time interval $9.0 \leq |\Omega|t \leq 10.0$. Right panel: Energy fluctuation as a function of $|\Omega|t$ for the same runs shown on the left panel; inset: basis-set conditioning factor $\varepsilon(t)$ for the corresponding curves.

Results obtained with the unitary SU(3) CCS method and by a direct diagonalization of the Hamiltonian (4.9) in the bosonic Fock basis are compared in Fig. 3. On the left panel, the occupation of the classically inaccessible b_3 mode is displayed for different basis-set sizes. On the right panel, the total energy expectation value (4.15) for each run is shown as well as the corresponding behavior of basis-set conditioning factors (see appendix A).

It is found that CCS results improve as more basis elements are included in the propagation, as expected – although there is some anomalous behavior, with the $M = 20$ run performing better than the $M = 30$ case. This is most likely due to the basis-set sizes involved, which are probably too small for a uniform convergence to be observed.

We also note that the quality of CCS results is intimately connected to conservation of total energy: the more accurate runs are also those in which energy is better conserved.

The most computationally expensive run, with $M = 60$ basis elements, led to an initial basis-set conditioning factor $\varepsilon(0) \approx 8.8 \times 10^7$, a value that diminished during the propagation. This behavior was observed in all cases – as shown in the inset of the right panel of Fig. 3 –, indicating spread of the classical trajectories. For this particular run ($M = 60$), excellent agreement between the CCS and exact solutions is found, except for slight discrepancies at $|\Omega|t \gtrsim 8.0$.

It should be noted that the propagation with $M = 60$ – which is quite a modest number of

basis elements for a problem with two degrees of freedom –, not only proved to be accurate[67] but also considerably faster than solving the 5151-dimensional quantum eigensystem. This gain in efficiency, at least for the model discussed here, drastically increases as more particles are added to the system, since the dimension of the SU(3) bosonic Fock space, given by $\frac{1}{2}(N+1)(N+2)$, grows rapidly with N. At the same time, the system becomes more classical as more particles participate in the dynamics, therefore making a trajectory-based approach more inviting.

Yet, despite these advantages, a reliable and positive way to check for the convergence of the CCS method still remains to be developed – the criterion of energy non-conservation being only indicative of accuracy loss during propagation. This represents a critical shortcoming when studying more complex systems for which there are no exact numerical results – or experimental data – available for comparison; for in those cases no precise statements about the system could be made based on CCS results alone.

V. SUMMARY AND CONCLUSIONS

In this work we have formulated a multiconfigurational, trajectory-guided quantum propagation method whose distinctive quality consists in employing generalized coherent states as basis elements. In this sense, the technique is seen as a natural extension of the coupled coherent states method of Shalashilin and Child[24–26] whereupon frozen Gaussians are replaced by more general configurations; at the same time, the main features of the original CCS are retained: quantum amplitudes obey an integro-differential equation with sparse coupling and present a smooth time dependence, owing to their oscillatory behavior being partially compensated by the classical motion of the basis elements and their action phases.

As pointed out in §II, no deep understanding of group-theory concepts is necessary, neither to derive the basic equations of the method nor to implement it numerically – in fact, we have seen that all geometrical quantities that enter the formulas can be straightforwardly evaluated from the coherent-state overlap function alone and that the discrete versions of the working equations do not differ in overall structure from their analogue expressions in the original CCS approach.

In §III, three versions of the method have been devised: continuum, non-unitary and unitary. The continuum version most evidently displays the novel elements due to the non-

Euclidean geometry associated with the generalized coherent-states and it serves primarily as a starting point for a number of possible analytical approximations. The non-unitary version, in turn, might be understood as a direct attempt to reproduce the continuum formulas by reducing phase-space integrals into finite sums. The unitary version, meanwhile, is the standard form of the method, being the most adequate for the majority of practical applications. We have also briefly discussed one weakness of this last version of the method which is the ill-conditioning of the overlap matrix. In that respect, we note that the basis-set sampling procedure that we propose – detailed in appendix A – is more appealing than the techniques used in previous CCS applications, for it assures an initially well-conditioned overlap matrix and hence stability of the amplitude equation (3.18), at least for short time propagation.

In §IV, we have illustrated the general aspects of the proposed approach with applications to simple models of many-boson systems, described in terms of SU(2) and SU(3) bosonic coherent states. One particular aspect, namely, the choice of appropriate phase-space variables for either sampling of initial conditions or grid construction, is found to be of great importance – coordinates chosen for these purposes must somehow reflect the intrinsic geometry of the coherent state under consideration, otherwise only a poor representation of the system is obtained. Moreover, the accuracy and efficiency of the method was established by comparing results against exact quantum calculations. Excellent agreement was observed and, in the triple-well system examined in §IV B, small discrepancies in the results were found to be correlated with energy non-conservation. These tests also allowed us to gain some insight regarding the domain of applicability of our formulas. A careful analysis of the fidelity in the double-well system studied in §IV A revealed that the CCS approach is best suited for describing the regime of large particle number, also identified as the semiclassical regime of that problem. This conclusion can in fact be extended for SU(n) bosonic systems in general. The same goes for the observations concerning the computational advantages of the method (over standard matrix diagonalization) when the number of particles is large; assertions which were made within the context of the triple-well problem.

Though we have exemplified the use of the method with SU(2) and SU(3) bosonic Hamiltonians, we emphasize that the formulation presented is by no means limited to these types of systems – in addition to the SU(n) fermionic coherent states discussed in §II C 4, other possible coherent-state parametrizations in terms of which the method could be readily im-

plemented were referenced throughout §I. Furthermore, the conclusion put forth in §IV, namely, that propagation of quantum states with the help of classically guided basis sets is better suited for describing systems in their semiclassical regime, is certainly expected to hold for any coherent-state representation that might be employed – provided one correctly interprets what 'semiclassical regime' means in each case.

A few words regarding the purely computational aspects of the method are in place. In the numerical calculations reported in this paper we have adopted the simplest possible strategy of implementation, which consists in propagating simultaneously the coherent-state trajectories and their corresponding amplitudes. But since trajectories evolve independently, an alternative approach would be to propagate them separately, storing the coherent-state coordinates at pre-determined time intervals and use this information afterwards in order to propagate the fully coupled amplitude equation – perhaps employing interpolation algorithms if coordinates are needed at intermediate instants.

This preliminary propagation of classical orbits could, of course, take full advantage of parallelization, especially if single basis elements are propagated with ease. It is however in those cases in which the very propagation of individual trajectories is a computationally demanding task – either because the system has an extremely large number of degrees of freedom or because no analytical expression for the Hamiltonian is available – that this 'two-stage' procedure would most definitely be the strategy of choice. In addition, it would allow for more sophisticated sampling techniques, since it would then be possible to select trajectories based on knowledge of their entire story, and not relying just on their initial proximity to the quantum state. Thus, for instance, one could identify orbits which, though unimportant at early stages of the propagation, give a significant contribution later on.

As a final and interesting remark, we note that the multiconfigurational Ehrenfest method,[69,70] as specifically designed for 'on-the-fly' non-adiabatic dynamics, can be obtained at once from the presented formalism as the particular case wherein each basis-set element is taken to be a composite coherent state consisting of a canonical part and an $SU(n)$ part with the particle-number parameter N set to unity.[68] In this picture, different 'diabatic' potential surfaces would be represented by the n single-particle states composing the $SU(n)$ coherent state; further extension to Born-Oppenheimer 'adiabatic' energy surfaces could be achieved without difficulty.

ACKNOWLEDGEMENTS

Appendix A: Basis set sampling

The basis set sampling procedure that we propose for the unitary CCS method (§III B 1) is outlined here. It applies to any type of coherent state once two geometry-dependent ingredients are provided: adequate sampling coordinates $q = f(z)$ – with a known inverse $z = f^{-1}(q)$ – and a weight distribution function $w(q)$ according to which these coordinates are to be randomly selected. The procedure assumes that the initial state is a coherent state, i.e. $|\psi_0\rangle = |z'\rangle$, in which case the initial coherent-state sampling coordinates $q' = f(z')$ must also be supplied.

The sampling strategy follows a very simple 'one-by-one' protocol, which draws inspiration from previously developed basis set conditioning techniques.[51] The procedure amounts to four steps:

(1) Take $|z'\rangle$ (the initial state itself) as the first basis element;

(2) Using the appropriate sampling coordinates q and weight function $w(q)$, randomly select a new basis element $z_j = f^{-1}(q_j)$ and temporarily add $|z_j\rangle$ to the basis set;

(3) Compute the overlap matrix Ω and evaluate its conditioning factor $\varepsilon = \lambda_{\max}/\lambda_{\min}$, where $\lambda_{\max}$ and $\lambda_{\min}$ are the largest and smallest eigenvalues of Ω, respectively.[72]

(4) If ε is less than some threshold value $\varepsilon_{\lim}$, accept $|z_j\rangle$ permanently adding it to the basis set, whose size increases by 1. Else, discard the selected basis element, in which case the basis-set size does not change. In either case, return to step (2);

The above procedure is then iterated until either a desired basis-set size is achieved or *saturation* occurs, meaning that the algorithm is unable to select a new $|z_j\rangle$ that satisfy the ε threshold condition (a certain maximum number of attempts may be specified). How fast saturation takes place will dependent upon the system's dimensionality, the threshold value $\varepsilon_{\lim}$, the coherent-state parameters and the details of the sampling distribution $w(q)$. Typically, we take $\varepsilon_{\lim} \sim 10^8 - 10^{12}$, and use a predetermined basis-set size below saturation,

thus ensuring a reasonably well-conditioned overlap matrix at initial time and hence the stability of the propagation (at least for sufficiently short times).

This sampling protocol requires the eigenvalues of the overlap matrix to be computed at every iteration. We point out, however, that this does not compromise the method's efficiency since the sampling is performed only once, before the actual propagation. Moreover, the overlap matrix typically does not grow too large; this assertion holds even for multidimensional systems, as long as the sampling distribution is kept sufficiently localized around the initial-state coordinate z' from where the most relevant contributions to the initial value representation formula are expected to originate. Finally, note also that the initial state $|z'\rangle$ is always included in the basis set; this is crucial for accuracy of short-time results and also secures that the initial norm is unity, regardless of how the remaining basis elements are distributed in phase space.

REFERENCES

[1] N. Makri. Time-dependent quantum methods for large systems. *Annual Review of Physical Chemistry*, 50(1):167, 1999.

[2] W. H. Miller and K. A. White. Classical models for electronic degrees of freedom: The second-quantized many-electron Hamiltonian. *The Journal of Chemical Physics*, 84(9):5059, 1986.

[3] A. Kirrander and D. V. Shalashilin. Quantum dynamics with fermion coupled coherent states: Theory and application to electron dynamics in laser fields. *Physical Review A*, 84(3):033406, 2011.

[4] F. Grossmann, M. Buchholz, E. Pollak, and M. Nest. Spin effects and the Pauli principle in semiclassical electron dynamics. *Physical Review A*, 89(3):032104, 2014.

[5] More recently, Grossmann *et. al.*[4] have investigated, in a semiclassical context, whether propagation with antisymmetrized basis states is essential for the description of electron scattering.

[6] H. Feldmeier and J. Schnack. Molecular dynamics for fermions. *Reviews of Modern Physics*, 72(3):655, 2000.

[7] T. Van Voorhis and D. R. Reichman. Semiclassical representations of electronic structure and dynamics. *The Journal of Chemical Physics*, 120(2):579, 2004.

[8] H. G. Solari. Glauber's coherent states and the semiclassical propagator. *Journal of Mathematical Physics*, 27(5):1351, 1986.

[9] H. G. Solari. Semiclassical treatment of spin system by means of coherent states. *Journal of Mathematical Physics*, 28(5):1097, 1987.

[10] T. F. Viscondi, A. Grigolo, and M. A. M. de Aguiar. Semiclassical propagator in the generalized coherent-state representation. Submitted, arXiv:1510.05952/quant-ph.

[11] Their discussion is based on a rough extension of Solari's semiclassical propagators[8,9] – a rigorous derivation of the generalized coherent-state propagator can be found in a recent work.[10]

[12] D. J. Thouless. Stability conditions and nuclear rotations in the Hartree-Fock theory. *Nuclear Physics*, 21:225, 1960.

[13] E. Deumens and Y. Öhrn. Time-dependent dynamics of a determinantal state. *Journal of Molecular Structure (Theochem)*, 199:23, 1989.

[14] E. Deumens, A. Diz, H. Taylor, and Y. Öhrn. Time-dependent dynamics of electrons and nuclei. *The Journal of Chemical Physics*, 96(9):6820, 1992.

[15] E. Deumens, A. Diz, R. Longo, and Y. Öhrn. Time-dependent theoretical treatments of the dynamics of electrons and nuclei in molecular systems. *Reviews of Modern Physics*, 66(3):917, 1994.

[16] T. Suzuki. Classical and quantum mechanical aspects of time-dependent Hartree-Fock trajectories. *Nuclear Physics A*, 398:557, 1983.

[17] H. Kuratsuji and T. Suzuki. Path integral approach to many-nucleon systems and time-dependent Hartree-Fock. *Physics Letters B*, 92:19, 1980.

[18] H. Kuratsuji and T. Suzuki. Path integral approach to many-body systems and classical quantization of time-dependent mean field. *Supplement of the Progress of Theoretical Physics*, 74-75:209, 1983.

[19] T. F. Viscondi and M. A. M. de Aguiar. Semiclassical propagator for SU(n) coherent states. *Journal of Mathematical Physics*, 52(5):052104, 2011.

[20] T. F. Viscondi and M. A. M. de Aguiar. Initial value representation for the SU(n) semiclassical propagator. *The Journal of Chemical Physics*, 134(23):234105, 2011.

[21] T. Van Voorhis and E. J. Heller. Nearly real trajectories in complex semiclassical dynamics. *Physical Review A*, 66(5):050501, 2002.

[22] T. Van Voorhis and E. J. Heller. Similarity transformed semiclassical dynamics. *The*

Journal of Chemical Physics, 119(23):12153, 2003.

[23] We note that the approximations to the generalized coherent-state path integral considered by Kuratsuji and Suzuki[18] – as well as specific formulations for Slater determinants[16,17] – are very much akin to the techniques develop in this paper.

[24] D. V. Shalashilin and M. S. Child. Time dependent quantum propagation in phase space. *The Journal of Chemical Physics*, 113(22):10028, 2000.

[25] D. V. Shalashilin and M. S. Child. Multidimensional quantum propagation with the help of coupled coherent states. *The Journal of Chemical Physics*, 115(12):5367, 2001.

[26] D. V. Shalashilin and M. S. Child. The phase space CCS approach to quantum and semiclassical molecular dynamics for high-dimensional systems. *Chemical Physics*, 304:103, 2004.

[27] W.-M. Zhang, D. H. Feng, and R. Gilmore. Coherent states: Theory and some applications. *Reviews of Modern Physics*, 62(4):867, 1990.

[28] The discussion is restricted to coherent states given in terms of analytical complex parametrizations.

[29] Entries of the vector z will be referenced by Greek letters α, β, γ.

[30] P. Kramer and M. Saraceno. *Geometry of the Time-Dependent Variational Principle in Quantum Mechanics*. Springer-Verlag, New York, 1981.

[31] T. F. Viscondi. PhD thesis, Universidade Estadual de Campinas, Instituto de Física Gleb Wataghin, Campinas, São Paulo, Brazil, 2013. Available in Portuguese.

[32] M. Baranger, M. A. M. de Aguiar, F. Keck, H. J. Korsch, and B. Schellhaaß. Semiclassical approximations in phase space with coherent states. *Journal of Physics A: Mathematical and General*, 34:7227, 2001.

[33] M. A. M. de Aguiar, S. A. Vitiello, and A. Grigolo. An initial value representation for the coherent state propagator with complex trajectories. *Chemical Physics*, 370:42, 2010.

[34] In the majority of applications involving coherent states and classical trajectories, the imaginary surface terms in A are canceled out by normalization factors. However, when *duplicated phase-space* trajectories are considered – i.e. when z and z^* are analytically continued in such a way that they become *completely independent* variables (thereby doubling the number of degrees of freedom in the system) –, the complex action A plays a prominent role, for its analytical properties are of the uttermost importance in those cases.[10,19,20,32,33]

[35] E. J. Heller. Frozen Gaussians: A very simple semiclassical approximation. *The Journal*

of Chemical Physics, 75(6):2923, 1981.

[36] E. J. Heller. Cellular dynamics: A new semiclassical approach to time-dependent quantum mechanics. *The Journal of Chemical Physics*, 94(4):2723, 1991.

[37] M. F. Herman and E. Kluk. A semiclassical justification for the use of non-spreading wavepackets in dynamics calculations. *Chemical physics*, 91:27, 1984.

[38] E. Kluk, M. F. Herman, and H. L. Davis. Comparison of the propagation of semiclassical frozen Gaussian wave functions with quantum propagation for a highly excited anharmonic oscillator. *The Journal of Chemical Physics*, 84(1):326, 1986.

[39] M. F. Herman. Dynamics by semiclassical methods. *Annual Review of Physical Chemistry*, 45:83, 1994.

[40] K. G. Kay. Integral expressions for the semiclassical time-dependent propagator. *The Journal of Chemical Physics*, 100(6):4377, 1994.

[41] K. G. Kay. The Herman-Kluk approximation: Derivation and semiclassical corrections. *Chemical Physics*, 322:3, 2006.

[42] F. T. Arecchi, E. Courtens, R. Gilmore, and H. Thomas. Atomic coherent states in quantum optics. *Physical Review A*, 6(6):2211, 1972.

[43] Owing to the finite width of the Gaussian functions employed as basis, CCS trajectories actually evolve under a smoothed-out classical Hamiltonian whose width-dependent terms are usually referred to as 'simple quantum corrections'.

[44] SU(n) fermionic coherent states should be contrasted with the antisymmetrized Gaussian wavepackets mentioned in §I. While the former are defined in terms of a finite set of underlying molecular spin-orbitals, thus providing a convenient description of the electronic structures of chemical systems, the latter are more adequate for representing localized fermions, such as protons and neutrons in the atomic nucleus,[6] or perhaps outer shell electrons in highly excited atoms.[3]

[45] I. Burghardt, H.-D. Meyer, and L. S. Cederbaum. Approaches to the approximate treatment of complex molecular systems by the multiconfiguration time-dependent Hartree method. *The Journal of Chemical Physics*, 111(7):2927, 1999.

[46] G. A. Worth and I. Burghardt. Full quantum mechanical molecular dynamics using Gaussian wavepackets. *Chemical Physics Letters*, 368:502, 2003.

[47] D. V. Shalashilin and I. Burghardt. Gaussian-based techniques for quantum propagation from the time-dependent variational principle: Formulation in terms of trajectories of

coupled classical and quantum variables. *The Journal of Chemical Physics*, 129(8):084104, 2008.

[48] For coherent states other than canonical, $|\langle z|z'\rangle|$ is no longer a Gaussian distribution, but is still localized in phase space.

[49] Latin letters j, k, l will be used for labeling basis-set elements and, for convenience, we henceforth abbreviate basis-set summations by omitting their ranges.

[50] K. G. Kay. The matrix singularity problem in the time-dependent variational method. *Chemical Physics*, 137:165, 1989.

[51] S. Habershon. Linear dependence and energy conservation in Gaussian wavepacket basis sets. *The Journal of Chemical Physics*, 136(1):014109, 2012.

[52] G. J. Milburn, J. Corney, E. M. Wright, and D. F. Walls. Quantum dynamics of an atomic Bose-Einstein condensate in a double-well potential. *Physical Review A*, 55(6):4318, 1997.

[53] T. F. Viscondi, K. Furuya, and M. C. de Oliveira. Generalized purity and quantum phase transition for Bose-Einstein condensates in a symmetric double well. *Physical Review A*, 80:013610, 2009.

[54] T. F. Viscondi, K. Furuya, and M. C. de Oliveira. Coherent state approach to the cross-collisional effects in the population dynamics of a two-mode Bose-Einstein condensate. *Annals of Physics*, 324(9):1837, 2009.

[55] K. Sakmann, A. I. Streltsov, O. E. Alon, and L. S. Cederbaum. Exact quantum dynamics of a bosonic josephson junction. *Phys. Rev. Lett.*, 103:220601, 2009.

[56] J. Schwinger. On angular momentum. In L. C. Biedenharn and H. Van Dam, editors, *Quantum Theory of Angular Momentum: A Collection of Reprints and Original Papers*, page 229. Academic Press, London, 1965.

[57] Throughout this section units are such that $\hbar = 1$.

[58] To compute the Hamiltonian (4.2), one could either use decomposition (2.23) to evaluate the required matrix elements of angular momentum operators or employ SU(2) generating functions.[27]

[59] R. Delbourgo. Minimal uncertainty states for the rotation and allied groups. *Journal of Physics A: Mathematical and General*, 10(11):1837, 1977.

[60] R. Delbourgo and J. R. Fox. Maximum weight vectors possess minimal uncertainty. *Journal of Physics A: Mathematical and General*, 10(12):L233, 1977.

[61] This can be verified by calculating the standard deviations of an appropriate quantum

phase-space distribution with respect to the angular coordinates θ and ϕ.

[62] L. G. Yaffe. Large N limits as classical mechanics. *Reviews of Modern Physics*, 54(2):407, 1982.

[63] T. F. Viscondi, K. Furuya, and M. C. de Oliveira. Phase transition, entanglement and squeezing in a triple-well condensate. *EPL (Europhysics Letters)*, 90:10014, 2010.

[64] T. F. Viscondi and K. Furuya. Dynamics of a Bose-Einstein condensate in a symmetric triple-well trap. *Journal of Physics A: Mathematical and Theoretical*, 44:175301, 2011.

[65] We note that in the triple-well model, the energy difference between the ground state and doubly degenerate excited states of the one-body Hamiltonian is $3\hbar\Omega$ – within the three-mode approximation these stationary states span the same eigenspace as the local modes associated with operators a_1, a_2 and a_3.[64] Also, in Eq. (4.9), we have made an additional simplification by excluding cross-collision terms, which arise from the interaction between bosons in different wells.

[66] This means that the smaller basis sets are embedded in the larger ones.

[67] No significant improvement of the results was observed for larger basis sets constructed with the same sampling parameters.

[68] As can be seen from Eq. (2.18), for the particular case of $N = 1$, the SU(n) coherent state reduces to $|z\} = |\phi_n\rangle + \sum_{\alpha=1}^{n-1} z_\alpha |\phi_\alpha\rangle$, where the occupation number representation has been replaced by 'first-quantized' notation, with $|\phi_\alpha\rangle$ being the single-particle orbital associated with the α-th mode. This is nothing but a standard decomposition of a quantum state in a finite basis of size n, only written without redundant parameters.

[69] D. V. Shalashilin. Nonadiabatic dynamics with the help of multiconfigurational Ehrenfest method: Improved theory and fully quantum 24D simulation of pyrazine. *The Journal of Chemical Physics*, 132(24):244111, 2010.

[70] K. Saita and D. V. Shalashilin. On-the-fly ab initio molecular dynamics with multiconfigurational Ehrenfest method. *The Journal of Chemical Physics*, 137(22):22A506, 2012.

[71] M. Galassi, J. Davies, J. Theiler, B. Gough, G. Jungman, M. Booth, and F. Rossi. *Gnu Scientific Library: Reference Manual*. Network Theory Ltd., 3rd edition, 2003.

[72] The overlap matrix is Hermitian and positive-definite, meaning that its eigenvalues are real and positive, though numerical diagonalization may produce null or very small negative eigenvalues. Alternatively, one could employ a singular value decomposition and carry on the sampling procedure using the singular values rather than the eigenvalues.